

Cite this article as: Li Yan, Liu Qi, Li Jucai, et al. Molecular Dynamics Simulation of Diffusion Behavior of Ti/Al Explosive Welding Interface[J]. Rare Metal Materials and Engineering, 2023, 52(06): 2017-2023.

ARTICLE

# Molecular Dynamics Simulation of Diffusion Behavior of Ti/Al Explosive Welding Interface

Li Yan<sup>1,2</sup>, Liu Qi<sup>1</sup>, Li Jucai<sup>2</sup>, Liu Cuirong<sup>1,2</sup>, Wu Zhisheng<sup>1</sup>

<sup>1</sup>School of Materials Science and Engineering, Taiyuan University of Science and Technology, Taiyuan 030024, China; <sup>2</sup>Preparatory Department, Modern College of Humanities and Sciences, Shanxi Normal University, Linfen 041000, China

**Abstract:** In order to reveal the diffusion behavior of Ti/Al interface, the molecular dynamics simulation was applied to study the microscopic diffusion mechanisms of Ti/Al explosive welding interface at the atomic scale. Molecular dynamics model of Ti/Al explosive welding spot was established by Materials Studio (MS). According to the physical process of explosive welding, the simulation of the collision was divided into two stages: the loading stage and the unloading stage. The mean square displacement (MSD), radial distribution function (RDF), and diffusion layer thickness were calculated by LAMMPS, and the diffusion behavior of interfacial atoms at different stages was reproduced by OVITO. Results show that in the loading stage of explosive welding, Ti and Al atoms do not diffuse but only vibrate at the equilibrium position, and the vibration of Al atoms is stronger than that of Ti atoms. The atomic diffusion only occurs in the unloading stage of the explosive welding process. The Ti-Ti bonding energy is too high to break. The Al-Al bonding energy is low, so it is easy to be damaged, resulting in vacancies, gaps and other defects, which promotes the deep diffusion of Ti atoms into the Al substrate lattice while hindering Al atoms from entering the Ti substrate lattice. The simulation result is basically in accordance with EDS experimental result.

**Key words:** explosive welding; molecular dynamics; Ti/Al interfaces; diffusion

Since Carl invented the explosive welding technology in 1944, the theoretical research and application of explosive welding technology have been greatly developed. According to incomplete statistics, more than 260 metal and alloy combinations can be welded together by explosive welding technology<sup>[1]</sup>. Explosive welding can realize the welding of various metals and composite the metals with extremely different material properties, such as lead and tantalum which have very different melting points, stainless steel and magnesium which are metallurgically insoluble materials, titanium and steel which have very different thermal expansion coefficients, lead and steel which have very different hardness. According to statistics, nearly 300 kinds of the same metal or dissimilar metal, metal and non-metal explosive welding combinations have been obtained<sup>[2]</sup>.

The melting point and thermal expansion coefficient of Ti/Al dissimilar metals differ greatly, and they have different crystal structures and limited miscibility, so they can produce

a variety of Ti/Al intermetallic compounds, while conventional fusion welding cannot achieve the reliable connection of Ti/Al. Explosive welding is a feasible method to prepare Ti/Al laminated composites. There are a lot of studies on the metallurgical bonding mechanism, process and structure of the Ti/Al explosive welding<sup>[3-7]</sup>, and a comprehensive analysis of the transient forming mechanism of Ti/Al explosive welding composite plates and tubes has been made by finite element numerical simulation<sup>[8-11]</sup>. However, the diffusion mechanism of Ti and Al at bonding interface and its influence on the product quality have been seldom satisfactorily explained at the atomic scale.

Diffusion is the most basic form of atomic motion<sup>[12-14]</sup>. If the diffusion behavior of atoms at the Ti/Al interface under the action of high-speed impact can be deeply discussed from the microscopic scale, it will be possible to achieve the perfect explosive welding composite theory system on the atomic scale. Molecular dynamics simulation has unique advantages

Received date: December 31, 2022

Foundation item: National Key Research and Development Program (2018YFA0707305); Major Science and Technology Projects of Shanxi Province (202101120401008); Key R&D Program of Shanxi Province (202102050201001); Linfen Key Research and Development Plan (2202); Science and Technology Innovation Project of Colleges and Universities in Shanxi Province (2022L628)

Corresponding author: Li Yan, Ph. D., Associate Professor, School of Materials Science and Engineering, Taiyuan University of Science and Technology, Taiyuan 030024, P. R. China, E-mail: yanli1988@tyust.edu.cn

Copyright © 2023, Northwest Institute for Nonferrous Metal Research. Published by Science Press. All rights reserved.

in revealing the physical and chemical phenomena on the atomic scale. Molecular dynamics can be used to observe microscopic phenomena that cannot be visible to the naked eye and detected by experimental equipment. Molecular dynamics has been applied to the analysis of diffusion problems at the interface of dissimilar materials. Chen et al<sup>[5]</sup> established a molecular dynamics model for the diffusion welding of copper (Cu) and aluminum (Al), and analyzed the influence of temperature, pressure and surface roughness on the atomic diffusion of the Cu/Al welding interface during diffusion welding. The simulation results show that at the simulated temperature of 600 K, there is almost no atom diffusion at the Cu/Al interface, and the materials on both sides maintain the original fcc structure. When the temperature is 650 K, the copper atom begins to diffuse towards the Al atoms, and the diffusion layer thickens with the increase in the diffusion temperature. Chen et al<sup>[6]</sup> also studied the diffusion behavior of Ni50Ti50-Cu under high-speed impact. For the first time, molecular dynamics method was applied to the study of alloy-metal diffusion, expanding the types of atoms from two to three. The LAMMPS program was used for programming calculation, and finally the atomic concentration distribution diagram of diffusion layer at different time was obtained. The simulation results were in great agreement with the EDS analysis results. Luo et al<sup>[7]</sup> studied the interfacial diffusion behavior of Cu/Al hot rolling diffusion composite based on molecular dynamics simulation, and analyzed the influence of temperature and pressure on interfacial atomic diffusion during the process of composite. The above studies indicate that molecular dynamics is an effective tool to study interfacial diffusion of dissimilar materials, which is useful for researchers to deeply understand the mechanism of interfacial atomic diffusion of dissimilar materials under different external conditions on the atomic scale.

## 1 Explosive Welding Experiment

Ti/Al explosive welding adopts parallel welding process, as shown in Fig. 1. Using 1 mm TA1 as cladding plate and Al-1060 with 3 mm in thickness as a substrate, the mixture of ANFO and RDX (5%–8%) was used as explosive. Then the explosive was ignited to realize explosive welding of titanium

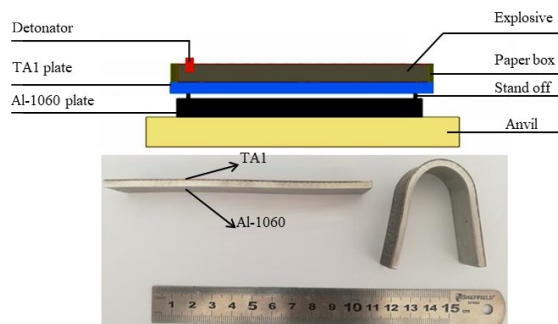


Fig.1 Experimental apparatus for explosive welding and Ti/Al composites

plate and Al plate.

## 2 Computational Model Method

### 2.1 Analysis tools

The molecular dynamics model of Ti/Al explosive welding spot was established by Materials Studio (MS), and the data file of the geometric model was obtained. The LAMMPS “in” program consistent with the physical process of explosive welding was compiled for solution calculation. Finally, visualization software OVITO was applied to analyze the simulation results.

### 2.2 Model establishment

Titanium has two kinds of structures at different temperatures: hexagonal close-packed structure (hcp) and body-centered cubic structure (bcc). The explosive welding is carried out at room temperature, at which titanium is in the state of hexagonal close-packed structure. The titanium and Al atoms models were selected from MS built-in material library. The specific parameters are shown in Table 1. Fig.2 shows the structure of Al and Ti atom cell.

Fig.3 shows the initial configuration of molecular dynamics simulation at the explosive welding joint of Ti/Al. The black box outside the model is for simulation, with the size of 6 nm (x)×6 nm (y)×50 nm (z). Pink represents the crystal supercell of Ti, with a size of 6 nm (x)×6 nm (y)×20 nm (z). There are

Table 1 Essential parameters of atoms

Atom	Lattice structure	Lattice constant/ $\times 10^{-1}$ nm	Atomic radius/ $\times 10^{-1}$ nm	Relative atomic mass
Ti	hcp	$a=b=2.9506$ $c=4.6788$	2	47.867
Al	fcc	$a=b=c=4.0495$	1.82	26.98

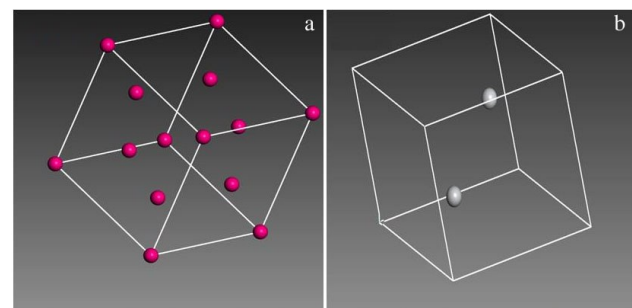


Fig.2 Cell structures of Al (a) and Ti (b)

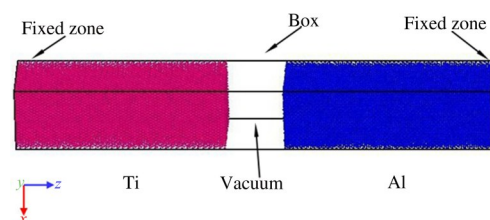


Fig.3 Initial configuration of model

60 lattice lengths in the  $x$ -axis and  $y$ -axis directions, 200 lattice lengths in the  $z$ -axis direction, and the number of supercell atoms is 42 588. The blue represents the crystal supercell of Al, with a size of 6 nm ( $x$ ) $\times$ 6 nm ( $y$ ) $\times$ 20 nm ( $z$ ). There are 60 lattice lengths in the  $x$ -axis and  $y$ -axis directions, 200 lattice lengths in the  $z$ -axis direction, and the number of atoms is 46 100. The whole system has a total of 88 688 atoms. The region between Ti and Al is a vacuum area.

### 2.3 Simulation settings

The choice of potential function is very important for molecular dynamics simulation. In this study, the Embedded Atom Method (EAM) developed by Zhou et al.<sup>[18]</sup> was adopted, which can describe the potential functions of 16 metal elements including Al and Ti. The simulation time step was set as 1 fs, and the numerical integral was calculated by shuffled frog leaping algorithm (SFLA). Periodic boundary conditions were set in the  $x$ -axis and  $y$ -axis directions of the initial configuration. In the  $z$ -axis direction, three layers of atoms in the top layer of Ti block and the bottom layer of Al block were set as fixed boundary conditions to simulate part of the macro crystal interacting with moving particles. In the  $z$ -axis direction, atomic layers move in time along with the whole simulation and were set as free boundary conditions. The initial thermal velocities of all atoms obey the Maxwell-Boltzmann distribution, and the Nose-Hoover hot bath is used as the temperature control technology in the simulation.

### 2.4 Simulation process

The explosive welding process is simplified to simulate the high-speed impact process between cladding plate and substrate. According to the numerical simulation results of explosive welding by Li et al.<sup>[19]</sup>, the explosive composite process of cladding plate and substrate belongs to the inclined collision. In the simulation, a certain transverse velocity and longitudinal velocity were applied to the cladding plate Ti to impact the Al block, and the diffusion phenomenon of the atoms at the Ti/Al interface after the collision was studied. Wronka<sup>[20]</sup>, Findik<sup>[21]</sup> and Yan<sup>[22]</sup> found through years of experimental and theoretical research that the spot position of explosive welding will experience a stress pulse at the moment of high-speed impacting between cladding plate and substrate, and the pressure value can reach dozens of GPa. After the combination of two welding spots, the pressure value of the welding spot will become zero. Therefore, the high-speed impact process of explosive welding can be regarded as a continuous loading and unloading process, and this method has been applied similarly in Ref.[23–25].

Energy minimization stage: after the explosive welding molecular dynamics model was established, the temperature with the Nose-Hoover hot bath control system is 300 K, and the Parrinello-Rahman method was used to control the pressure of the system to 0 MPa. In the isothermal-isobaric ensemble (NPT), the energy is minimized so that the system can reach the equilibrium state by relaxation of 1 million steps at 1 fs step size.

Loading stage: after the energy minimization relaxation is

completed, a certain speed is applied to the Ti block to make it collide with the fixed Al block, simulating the collision process between the substrate and the cladding plate in the explosive welding process. The actual detonation velocity of the mixed explosive of ANFO and RDX (5%–8%) selected in the experiment is determined to be 3800–4100 m/s, and the cladding plate speed is calculated according to the following formula:

$$V_p = 2V_d \sin \frac{\beta}{2} \quad (1)$$

where  $V_p$  is the velocity of cladding plate,  $V_d$  is the explosive detonation speed, and  $\beta$  indicates the dynamic bend angle of cladding plate. The dynamic bend angle should be taken at 5°–25°. The  $z$ -axis direction velocity and  $x$ -axis direction velocity of the cladding plate are 1500 and 700 m/s, respectively for simulation calculation<sup>[26–27]</sup>.

The collision of explosive welding is a transient process, about  $10^{-15}$  s. This process takes a very short time and the heat generated will not be transferred. It can be regarded as an adiabatic process. Therefore, the collision stage is set under the micro-canonical ensemble (NVE), and the loading process is relaxed by 1 million steps, that is, the loading stage is 1000 ps.

Unloading stage: Yan et al.<sup>[22]</sup> mentioned in their study that the temperature of the system decreases slowly in the unloading stage, so the unloading stage can be treated as an isothermal process. After relaxation in the loading stage, the temperature remains unchanged after loading, and the pressure of the system changes to 0 MPa to simulate the physical process of stress pulse decline during the collision. The simulated ensemble changes from NVE in the loading stage to NPT, and the relaxation in the unloading process is 1 million steps, namely 1000 ps in the unloading stage.

## 3 Results and Discussion

Fig. 4 shows the atomic configuration diagram of OVITO output at different time. At the initial stage of 0 ps, Ti and Al atoms are separated by a vacuum. At 1000 ps, the loading

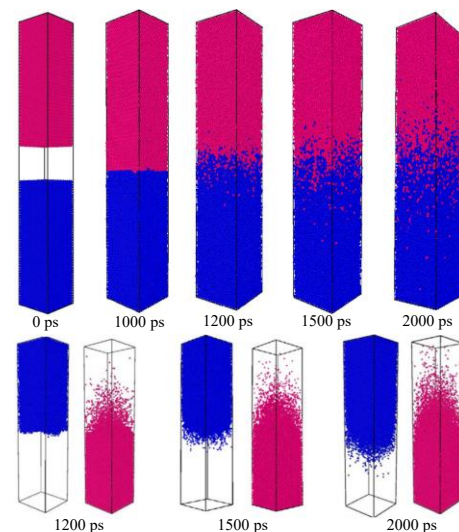


Fig.4 Atomic distribution at different time

stage is completed, and the two kinds of atoms do not diffuse into each other, because under the extremely high pressure in the loading stage, the density of the crystal increases, the space of atomic motion shrinks, and the long-range diffusion is difficult. After unloading, obvious diffusion zone appears at the Ti/Al interface after holding for 200 ps. After 500 ps unloading, the thickness of the diffusion zone increases, and the two kinds of atoms mix with each other. The Ti atoms diffuse more to the Al side, while the Al atoms diffuse less to the Ti side. With the extension of the unloading insulation time, Ti atoms and Al atoms continue to diffuse to each other, and the thickness of the diffusion layer increases. According to the basic rule that the higher the melting point, the stronger the metallic bonds, the melting point of Ti and Al is 1933 and 933 K, so the bonding ability between Ti atoms is stronger than that between Al atoms. Therefore, higher energy is required to destroy the bonding of Ti atoms. In contrast, Al atoms are easier to be destroyed, resulting in vacancies, gaps and other defects. These vacancies and gaps can be used as diffusion channels for atoms, which is conducive to the diffusion of Ti atoms into the Al lattice. Therefore, Ti atoms at the interface diffuse more to the Al side, while Al atoms diffuse less to the Ti side.

### 3.1 Mean square displacement

Fig. 5a shows the mean square displacement (MSD) curves of Ti atoms and Al atoms in the loading stage (1000 ps). The dotted line is the MSD curve of Ti atoms, and the red solid line is the MSD curve of Al atoms. At the end of loading, the MSD curves of Ti and Al atoms are parallel to the time axis. The MSD of Ti atoms vibrates around  $5 \text{ nm}^2$ , and the MSD of Al atoms vibrates around  $230 \text{ nm}^2$ . This phenomenon shows that in the loading stage, the Ti and Al atoms in the system do not diffuse, but only vibrate at the equilibrium position, and the vibration of Al atoms is much stronger than that of Ti atoms.

Fig. 5b shows the MSD curves of Ti and Al atoms during the unloading stage. It can be seen that the MSD of the two kinds of atoms increases linearly with the increase in time, indicating that both Ti and Al atoms have diffusion during the unloading stage. After the unloading stage (2000 ps), the maximum MSD of Al atoms is  $100 \text{ nm}^2$ , and that of Ti atoms is  $20 \text{ nm}^2$ . The slope of the MSD curves represents the

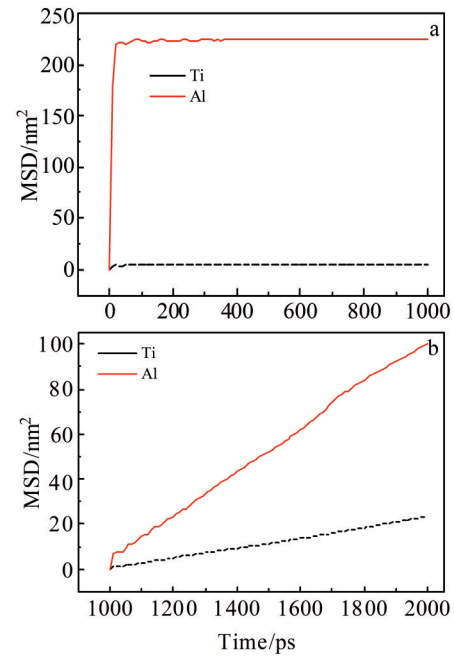


Fig. 5 MSD of Ti atoms and Al atoms along the  $z$ -axis direction: (a) loading stage and (b) unloading stage

diffusion coefficient of the atom. The diffusion rate of the Al atoms is higher than that of the Ti atoms.

### 3.2 Radial distribution function

Fig. 6a and 6b show the radial distribution function curves of Ti-Ti atomic pairs and Al-Al atomic pairs. The initial configuration of Ti atoms is a regular hexagonal close-packed (hcp) lattice structure, and the initial configuration of Al atoms is a regular face-centered cubic (fcc) lattice structure. At 0 ps, the radial distribution function curves of Ti-Ti atomic pairs and Al-Al atomic pairs show high and narrow shape, indicating the characteristics of long-range order, which indicates that the atoms have regular crystal structure before collision. After 1000 ps loading, the radial distribution function curves of Ti-Ti atomic pairs and Al-Al atomic pairs become shorter and wider, indicating that Ti/Al atomic pairs are no longer a complete regular crystal structure under high-speed impact. The kinetic energy of Ti atoms is transformed into the deformation energy of two atoms, and the two atoms

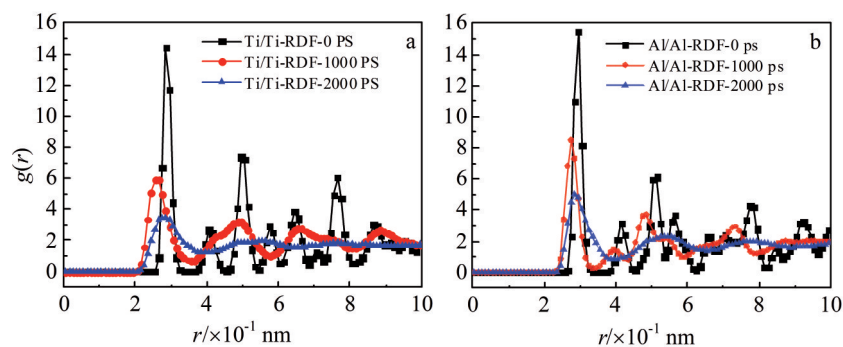


Fig. 6 Radial distribution functions of different stages for Ti/Ti (a) and Al/Al (b)



undergo plastic deformation. The irregular motion of the atom is intensified, leaving the original equilibrium position, which leads to a disorderly shift in structure. At 2000 ps, the radial distribution function curves of Ti-Ti atomic pairs and Al-Al atomic pairs become shorter and wider than those after loading. The radial distribution function shows several fading passivation peaks. After reaching the peak value, the function value gradually tends to  $2 \times 10^{-1}$  nm. This is because after unloading, the mutual diffusion of Ti atoms and Al atoms increases the degree of disorder of atoms in the diffusion area, i.e. the radial distribution function curve becomes shorter and wider, and the peak value decreases.

### 3.3 Thickness of diffusion layer

In order to further quantitatively analyze the thickness of the atomic diffusion layer at the Ti/Al interface, the “chunk” command in LAMMPS was used to calculate the concentration distribution curve along the z-axis direction at the Ti/Al interface. The specific method is: divide the whole system into 65 parts along the z-axis and count the number of atoms in each layer after loading and unloading. Fig. 7 shows the relative content distribution of atoms at the Ti/Al interface

under collision conditions. The diffusion region is defined as the area near the interface where the relative content of Ti and Al atoms exceeds 5%. As can be seen from Fig. 7, after the loading, the thickness of diffusion layer of Ti and Al atoms is  $5 \times 10^{-1}$  nm, and there is basically no diffusion layer. After unloading, with the extension of time, the thickness of diffusion layer gradually becomes thicker, which is consistent with the results observed in Fig. 4.

### 3.4 Analysis of interface elements

Fig. 8 presents the vertical Ti/Al explosive welding composite interface by EDS line scanning. The diffusion curve of the two elements at the interface shows an “X” shape, and the content of the two atoms has a continuous and smooth transition, indicating that Ti and Al elements diffuse to each other during the explosive welding process, and the two metals have achieved metallurgical bonding. The thickness of the Ti/Al explosive welding diffusion layer is about 8  $\mu\text{m}$ .

Fig. 9 shows EDS mappings of two elements at the Ti/Al interface. It can be seen that the two elements diffuse to each other at the interface, and the amount of Ti element diffused to the Al matrix is greater than that of Al element diffused to the

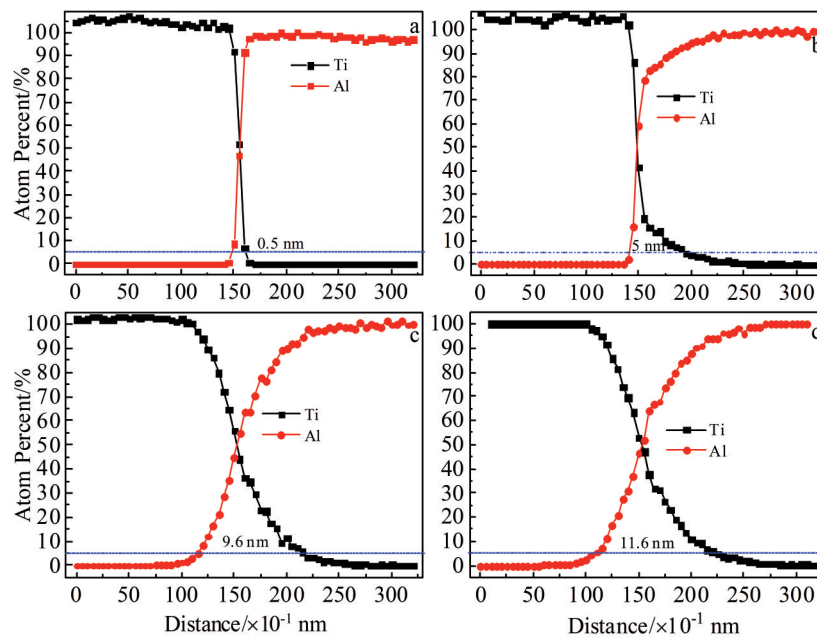


Fig.7 Concentration of Al and Ti atoms along the z-axis direction: (a) 1000 ps, (b) 1200 ps, (c) 1500 ps, and (d) 2000 ps

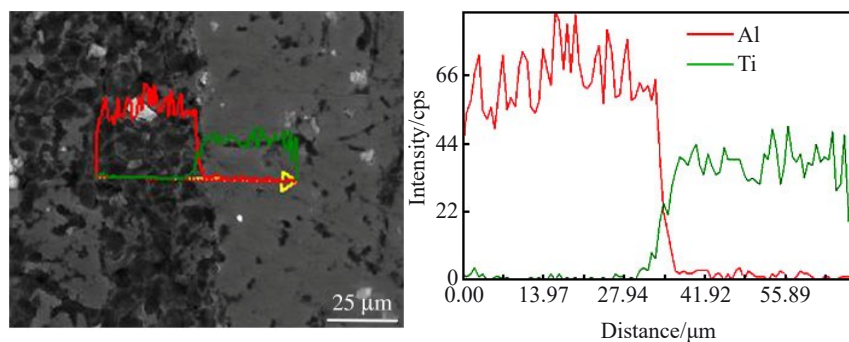


Fig.8 EDS line scanning along the arrow direction

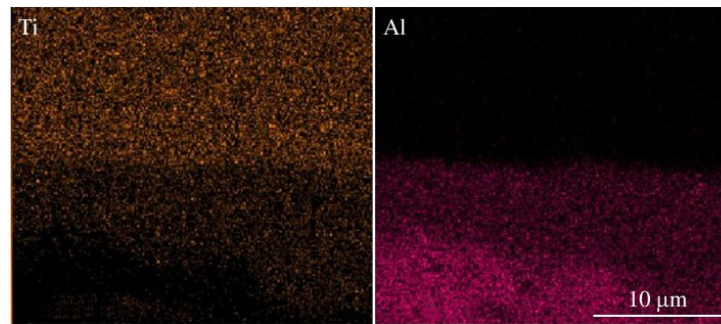


Fig.9 EDS mappings of element Ti and Al near the interface position

Ti matrix. The scanning results of interface elements are consistent with the simulation results of molecular dynamics.

Based on the analysis of the atom distribution at the Ti/Al interface and the MSD curves of Ti and Al, it can be concluded that at the Ti/Al interface, Al atoms diffuse to the Ti side with a faster rate, but it is difficult to enter the Ti lattice. The Ti atoms diffuse at a slower rate, but it can penetrate into the Al lattice. This phenomenon is similar to the simulation results of interfacial diffusion of other dissimilar metal systems<sup>[28-30]</sup>.

#### 4 Conclusions

1) The atoms at the Ti/Al interface do not diffuse during the loading stage of explosive welding, but the diffusion occurs during the unloading stage.

2) The kinetic energy of explosive welding Ti atoms is converted into the deformation energy of the whole system, the system structure changes from long-range order to disorder, and the radial distribution function changes from high and narrow to low and wide in shape.

3) The Al atoms at the Ti/Al explosive welding interface diffuse to the Ti side at a faster rate, but it is difficult to enter the lattice of Ti. Ti atoms diffuse at a slower rate, but can diffuse deep into the Al lattice.

#### References

- 1 Bi Z X, Li X J, Wu Y et al. *Rare Metal Materials and Engineering*[J], 2022, 51(10): 3611
- 2 Zu G Y. *Rare Metal Materials and Engineering*[J], 2017, 46(4): 906
- 3 Xia H B, Wang S G, Ben H F. *Materials & Design*[J], 2014, 56(4): 1014
- 4 Khausto S V, Pai V V, Lukyanov Y L et al. *Thermal Science and Engineering Progress*[J], 2022(30): 30
- 5 Bian M, Huang X, Saito N et al. *Journal of Alloys and Compounds* [J], 2022, 898: 162 957
- 6 Wu X, Shi C, Feng K et al. *Materials Research Express*[J], 2021, 8(9): 96 503
- 7 Solecka M , Sebastian Mróz, Petrzak P et al. *Archives of Civil and Mechanical Engineering*[J], 2022, 23(1): 39
- 8 Yu H, Lu C, Tieu A K et al. *Materials Science & Engineering A*[J], 2016, 660: 195
- 9 Ren B , Tao G , Wen P et al. *International Journal of Refractory Metals and Hard Materials*[J], 2019, 84: 105 005
- 10 Guo X Z, Tao J, Yuan Z et al. *Rare Metal Materials and Engineering*[J], 2012, 41(1): 139 (in Chinese)
- 11 Feng J, Liu R, Liu K et al. *Journal of Applied Physics*[J], 2022(2): 131
- 12 Fronczek D M, Wojewoda-Budka J, Chulist R et al. *Materials & Design*[J], 2016, 91: 80
- 13 Lazurenko D V, Bataev I A, Mali V I et al. *Materials & Design*[J], 2016, 1021: 122
- 14 Jilin Xie, Wentao Zhang, Yuhua Chen et al. *Materials Characterization*[J], 2022, 194: 112 462
- 15 Chen S, Ke F, Min Z et al. *Acta Materialia*[J], 2007, 55(9): 3169
- 16 Chen S Y, Wu Z W, Liu K X. *Chinese Physics B*[J], 2014, 23(6): 446
- 17 Luo L, Wang B F, Li L R. *Heat Treatment Technology and Equipment*[J], 2011, 32(2): 6 (in Chinese)
- 18 Zhou X W, Johnson R A, Wadley H N G. *Physical Review B*[J], 2004, 69(14): 1124
- 19 Li Y, Liu C, Yu H et al. *Metals*[J], 2017, 7(10): 407
- 20 Wronka B. *Journal of Materials Science*[J], 2010, 45(13): 3465
- 21 Findik F. *Materials & Design*[J], 2011, 32(3): 1081
- 22 Yan H H, Qu Y D, Li X J. *Combustion Explosion & Shock Waves*[J], 2008, 44(4): 491
- 23 Chen S Y, Wu Z W, Liu K X et al. *Journal of Applied Physics*[J], 2013, 113(4): 1333
- 24 Fan M Y, Guo X Z, Cui S Q et al. *Rare Metal Materials and Engineering*[J], 2017, 46(3): 770 (in Chinese)
- 25 Zhang T T, Wang W X, Zhou J et al. *Acta Metallurgica*[J], 2017, 52(1): 1
- 26 Li Y, Li Y B, Liu C R et al. *Pressure Vessel Technology*[J], 2021, 38(5): 8 (in Chinese)
- 27 Chen X, Inao D, Tanaka S et al. *Transactions of Nonferrous Metals Society of China*[J], 2021, 31(9): 2687
- 28 Luo N, Shen T, Xiang J X et al. *Rare Metal Materials and Engineering*[J], 2018, 47(10): 3238 (in Chinese)

- 29 Li C, Li D, Tao X et al. *Calphad-Computer Coupling of Phase Diagrams & Thermochemistry*[J], 2015, 51(6): 396
- 30 Chen S D, Soh A K, Ke F J. *Scripta Materialia*[J], 2005, 52(11): 1135

## 钛/铝爆炸焊接界面扩散行为分子动力学模拟

李 岩<sup>1,2</sup>, 刘 琪<sup>1</sup>, 李聚才<sup>2</sup>, 刘翠荣<sup>1,2</sup>, 吴志生<sup>1</sup>

(1. 太原科技大学 材料科学与工程学院, 山西 太原 030024)

(2. 山西师范大学现代文理学院 转设筹备处, 山西 临汾 041000)

**摘 要:** 为揭示钛/铝爆炸焊接界面原子的扩散行为, 采用分子动力学模拟从原子尺度分析了钛/铝爆炸焊接界面原子的微观扩散机理。利用 Materials Studio 建立了钛/铝爆炸焊接焊点处的分子动力学模型, 结合爆炸焊接的物理过程, 将爆炸焊接过程分为加载和卸载 2 个阶段, 通过 LAMMPS 程序计算了爆炸焊接钛、铝原子的均方位移、径向分布函数、扩散层厚度等, 利用 OVITO 软件再现了不同阶段界面原子的扩散行为。在爆炸焊接加载阶段, 钛、铝原子不发生扩散, 只在平衡位置做振动, 铝原子振动要比钛原子振动强。爆炸焊接卸载开始时, 钛、铝原子发生互扩散。钛/钛原子键能高, 不易破坏, 铝/铝原子键能低, 容易破坏产生空位、间隙等缺陷, 有利于钛原子深入扩散到铝晶格内部, 但铝原子难以进入钛的晶格内部。采用扫描电镜和 EDS 能谱表征了钛/铝爆炸焊接复合材料界面元素分布, 与模拟结果有很好的 consistency。

**关键词:** 爆炸焊接; 分子动力学模拟; 钛/铝界面; 扩散

**作者简介:** 李 岩, 男, 1988 年生, 博士, 副教授, 太原科技大学材料科学与工程学院, 山西 太原 030024, E-mail: yanli1988@tyust.edu.cn